Eur. Phys. J. D **2**, 157–163 (1998)

THE EUROPEAN PHYSICAL JOURNAL D

Observation of bistability in a perturbed magneto-optical trap

D. Wilkowski[a], J.C. Garreau[b], and D. Hennequin[c]

Laboratoire de Physique des Lasers, Atomes et Molécules, Centre d'Études et de Recherches Laser et Applications, Université des Sciences et Technologies de Lille, 59655 Villeneuve d'Ascq Cedex, France

Received: 5 November 1997 / Revised: 13 March 1998 / Accepted: 24 March 1998

Abstract. We report on the experimental observation of bistability in a magneto-optical trap perturbed by a focalized laser beam. This bistability is theoretically interpreted by studing the atomic losses induced by the perturbing beam. Comparison with a Monte Carlo model allows us to deduce the trap capture velocity *along* the perturbing beam.

PACS. 32.80.Pj Optical cooling of atoms; trapping – 42.50.Vk Mechanical effects of light on atoms, molecules, electrons, and ions – 42.65.Sf Dynamics of nonlinear optical systems; optical instabilities, optical chaos and complexity and optical spatio-temporal dynamics

1 Introduction

The dynamics of the magneto-optical trap (MOT) is a subject of great interest. The very first experiments of atom trapping in a MOT have shown much lower temperatures and much larger cloud sizes than expected on the basis of simple theories. The first theoretical efforts were then concentrated in understanding why the equilibrium temperature was so low (of the order of a few microkelvins), and lead to the polarization-dependent mechanisms of the Sisyphus effect or the alignment effect [1]. Two kinds of collective effects have also been identified [2,3]. The first one is the so-called "shadow effect": due to the optical thickness of the atomic cloud, different atoms inside the cloud see different beam intensities, and this generates a force pushing the atoms one against the other, contributing thus to *reduce* the size of the cloud. In the usual MOT configuration using three retro-reflected beams, this effect also shifts the center of mass of the atomic cloud with respect to the center of the trap, that is, the zero-magnetic field point. As we will see, this displacement plays an essential role in the phenomenon studied in the present paper. The second collective effect is called "multiple scattering", and arises from the fact that an atom inside the cloud can scatter a photon emitted by another atom of the cloud. This effect can be modelized as an effective repulsive coulombian interaction among the atoms and thus contributes to *increase* the size of the atomic cloud. In fact, the abnormally large cloud size has been attributed to this effect.

Aside the collective effects discussed above, unusual spatial cloud structures have been observed, in the case of misaligned traps, and theoretical explanations based on the generation of vortex forces by the beam misalignment have been proposed [4,5].

Many works have been devoted to the dynamics of the atomic cloud captured in a vapor-cell MOT [6–8], and to MOTs with only one atom [9]. There have been relatively few experimental results concerning properties of the MOT as essential as its capture velocity, *i.e.* the maximum velocity allowed for an atom to be trapped into the MOT. In particular, the evident anisotropy of the MOT was never studied to our knowledge.

In this paper, we voluntarily perturbed a cloud of cold atoms with a highly focalized laser beam, the perturbing beam (PB), and we show that, under certain conditions, the measurement of the population of the cloud as the intensity of this beam is swept reveals a bistability phenomenon. The study of one of the transition points in the bistability cycle allows us to deduce the trap capture velocity along the PB.

The paper is organized as follows: In Section 2 we briefly describe the experimental set-up and present measurements of the bistability cycle and in particular of the dependence of one of the turning points on the detuning of the perturbing beam. We measure an important effect: the displacement of the center of mass of the atomic cloud as a function of its population, and we interpret this effect as due to the shadow effect. In Section 3 we introduce a simple model that clearly puts into evidence the physical mechanism leading to the bistability, although it does not allow a quantitative description of the phenomenon. A quantitative approach, introduced in Section 4, is a numerical Monte-Carlo model that describes the interaction of the perturbing beam with the cold atoms. This model

[a] *Present address:* Dept. di Fisica, Università degli Studi di Pisa, Piazza Torricelli, 2, 56126 Pisa, Italy
e-mail: wilkow@mailbox.difi.unipi.it
[b] e-mail: garreau@lsh.univ-lille1.fr
[c] e-mail: daniel@lsh.univ-lille1.fr

allows us to deduce the trap capture velocity along the perturbing beam. Finally, Section 5 concludes our work.

2 Experimental set-up and results

We work with the cesium D2 line ($\lambda = 852$ nm). The MOT is formed by three mutually orthogonal retro-reflected laser beams with orthogonal circular polarization, whose intensity I_T can be chosen between zero and four times the saturation intensity for the cesium ($I_S = 2.2$ mW/cm^2). The trapping is obtained by applying a magnetic field gradient of 14 G/cm. The MOT detuning δ_T can be varied from 0 to -6Γ ($\Gamma = 2\pi \times 5.3$ MHz is the natural width of the transition). The maximum population of the trap is $N = 2 \times 10^8$ atoms, in a volume of about 1 mm^3. The trapping diode laser is injected by a master diode laser, which is locked on the saturated absorption profile of the cesium line. The master diode is also used to inject the additional laser diode that supplies the independent beam used to perturb the trap, the perturbing beam (PB). This beam is coplanar with two arms of the magneto-optical trap (Fig. 1). Let us define spatial axes (x, y, z) along the arms of the trap, with z being the vertical axis and the origin coinciding with the zero magnetic-field point, that we shall call the *center of the trap*. The PB defines another spatial frame (x', y', z). We choose the x' axis along the PB, making an angle θ with the x axis of the trap, whereas the transverse direction with respect to the PB defines the y' axis. The vertical axes are the same in both frames. The PB is focalized to a waist of 10 μm at the zero-magnetic field point, and its typical power is a few mW, which gives Rabi frequencies as high as 1000Γ. An acousto-optical modulator allows us to sweep the detuning δ_P of the PB with respect to resonance. The atomic cloud is imaged onto two CCD cameras, one in a direction close to the axis of the PB and the other orthogonally to this axis, along the y' axis. The population is monitored by focalizing the fluorescence light of the trap collected over a solid angle of 0.2 sr onto a photodiode.

A crucial role in the bistability phenomenon is played by the coupling between the population and the displacement (due to the shadow effect) of the center-of-mass (CM) of the atomic cloud with respect to the center of the trap. This coupling originates in the fact that each arm of the trap is formed by a retro-reflected laser beam: the "on-going" beam is absorbed by the atoms into the cloud, then retro-reflected before passing again inside the cloud. The back-reflected beam is thus always weaker than the on-going beam, creating an imbalance in the radiation pressure seen by a given atom into the cloud. The consequence is a net force pushing the atoms of the cloud in the direction of the retro-reflection mirror until the effect of the restoring force generated by the magnetic-field gradient equilibrates the radiation pressures. In three dimensions, the CM of the atomic cloud is displaced along the bisector of the tri-orthogonal trap arms. One easily understands that this displacement is proportional to the optical thickness of the cloud, and one expects it to increase with the cloud population, which can be verified experimentally. A maximum displacement is observed for a detuning of the trap around -2.5Γ.

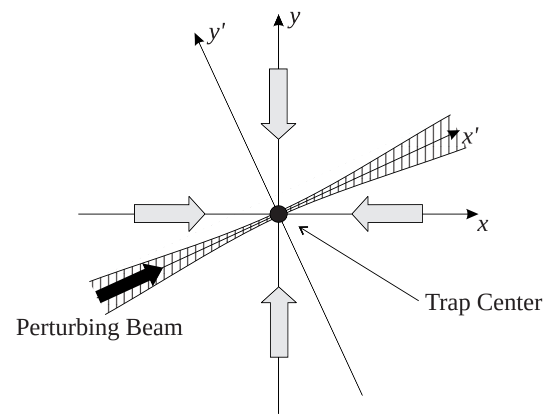

Fig. 1. Experimental set-up. The PB is contained in the plane formed by the x and y-axes of the MOT, and makes an angle θ with the x-axis. The z-axis is perpendicular to the plane of the figure.

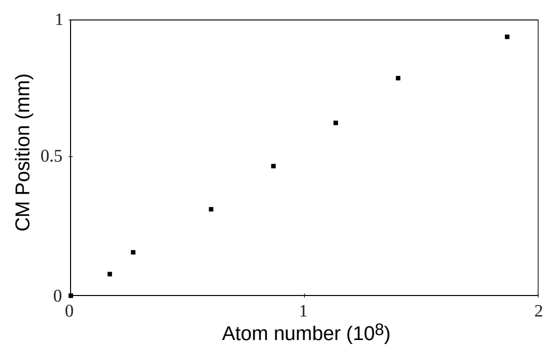

Fig. 2. Experimental measurement of the position of the center-of-mass of the atomic cloud as a function of the population, in the absence of the perturbing beam. There is an almost linear relation between the two quantities. The parameters of the trap are $\delta_T = -1.5\Gamma$, $I_T = 3I_s$. The mean slope is 0.5 mm/10^8 atoms, corresponding to $a = 2.05$, where a is a parameter defined in equation (16).

We experimentally studied the dependence of the CM position on the trap population in the absence of the PB. This is done by imaging the atomic cloud over a "four-quadrants" photodiode. The result is shown in Figure 2, revealing an almost linear relation between the CM position and the population. This result will be useful in the following of the paper.

We show in Figure 3 a typical bistability cycle observed in our experiment by monitoring the fluorescence of the cloud as a function of the perturbing beam intensity I_P. We start from a low intensity PB, and consequently from a highly-populated trap, corresponding to the upper branch of the bistability cycle. The atomic cloud is then displaced with respect to the center of the trap, and thus with respect to the PB. As a consequence, the PB interacts essentially with the periphery of the atomic cloud (see Fig. 4a), and has a limited efficiency in expelling atoms

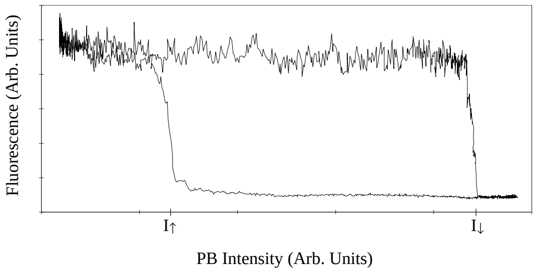

Fig. 3. Experimentally observed bistability cycle obtained by sweeping the intensity of the perturbing beam and simultaneously recording the atomic cloud fluorescence. Parameters are $\delta_T = -1.5\Gamma, I_T = 4I_s, \delta_P = -3.9\Gamma$.

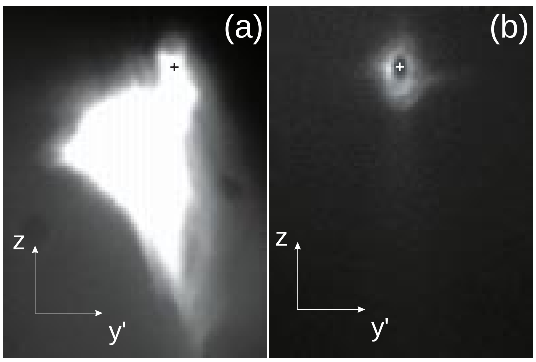

Fig. 4. CCD camera images of the atomic cloud in the plane orthogonal to the perturbing beam. (a) Trap in the high-population state. (b) Trap in the low-population state. The crosses show the location of the trap center.

from the cloud. When the intensity of the PB reaches a transition value $I_\downarrow$, we observe a strong decreasing of the fluorescence, corresponding to the transition to the lower branch of the cycle. Then one sees, in the plane orthogonal to the PB, a ring-shaped atomic cloud, with a hole at the center (Fig. 4b). At the same time, in the plane parallel to the PB, a jet of atoms pushed out of the cloud appears (Fig. 5), showing that important losses are now induced by the PB. An important point to be noted is that the CM of the atomic cloud now coincides with the PB. This fact is not surprising: as the system is now in its low population branch, its optical thickness is low, and so is the shadow effect. At the same time, this also explains the increased efficiency of the PB in expelling atoms from the cloud: it crosses the center of the atomic cloud rather than its periphery, as it occurred when the system was in the upper branch.

As the intensity of the perturbing beam is decreased from its maximum value, we observe a decreasing of the diameter of the hole at the center of the cloud, together with a progressive disappearance of the atomic jet along the perturbing beam. Finally a transition from the lower to the upper branch of the cycle occurs, but at an intensity $I_\uparrow$ *lower* than $I_\downarrow$, giving rise to the characteristic shape of a bistability cycle. We experimentally verified that there

Fig. 5. CCD camera image of the trap in its low-population state in a plane parallel to the perturbing beam, showing the jet of atoms expelled from the trap.

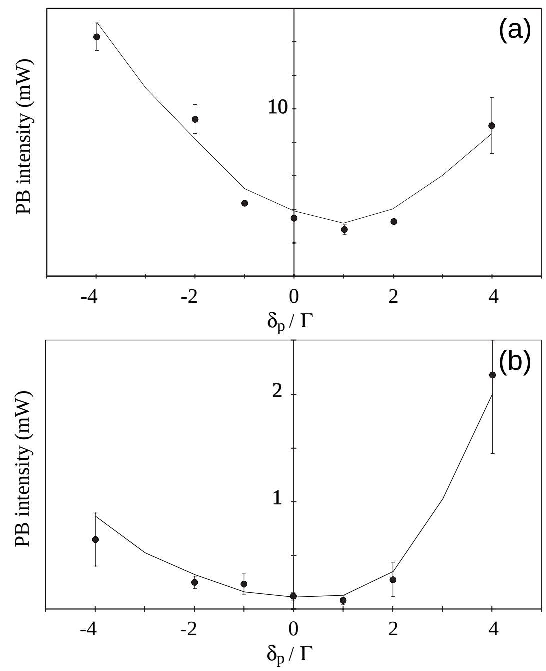

Fig. 6. Perturbing beam intensity $I_\downarrow$ corresponding to the up-down transition point as a function of the detuning of the PB. For both graphs the parameters of the trap are $I_T = 4\Gamma$, $\delta_T = -1.5\Gamma$. (a) $\theta = 23°$, (b) $\theta = 35°$. The solid curves correspond to the numerical fit described in Section 4. The fits give the following values: (a) $v_c(23°) = 49$ m/s and $D_{th}(23°) = 0.255$. (b) $v_c(35°) = 12$ m/s and $D_{th}(35°) = 0.254$.

is no bistability if the PB is displaced far enough from the center of the trap.

We performed a study of the transition point $I_\downarrow$ as a function of the detuning δ_P of the perturbing beam, for two values of the angle θ. The result is presented in Figure 6. We found that the transition intensity is lower if this angle approaches 45°, which is not surprising as the trap confinement is weaker along the bisectors of the trap beams. We choose to study the up-low rather than the low-up because it corresponds to a initial cloud shape not too different from an unperturbed MOT. It is relatively homogenous and easier to modelize. As we will see in Section 4, a numerical model describing the interaction of the trapped atoms with the PB allows us to deduce the trap capture velocity along the perturbing beam.

In the next section we will introduce a theoretical model that can explain the bistability and gives a simple physical interpretation of this phenomenon.

3 Theoretical model

In this section we develop a simple theoretical model to put into light the physical origin of the bistability phenomenon. This model is not intended to describe in detail the interaction of the perturbing beam with the trapped atoms, but to show how bistability arises from the losses induced by the PB and from the dependence of the CM position on the population of the atomic cloud.

Our one-dimensional model is based on the following assumptions:

1. The population N of the trap is governed by a "feed-loss" equation:
$$\frac{dN}{dt} = R - bN \tag{1}$$
where R is the feed term and b is the total loss coefficient. This form has been widely used in the literature to describe the global population evolution in MOTs (see, *e.g.* [6]).
2. The perturbing beam removes atoms from the trap, increasing the losses. The equilibrium population N_s of the trap is determined by the equilibrium between the feed term and the losses. The loss term includes both the losses induced by the PB, $b_P(I_P, \delta_P)$, and the normal losses of the trap in the absence of the PB, b_0:
$$N_s = \frac{R}{b} = \frac{R}{b_0 + b_P}\cdot \tag{2}$$
3. The efficiency of the PB in inducing losses depends on the effective number of atoms interacting with it. As the PB is focalized into the trap to a waist that is about a hundred times smaller than the size of the atomic cloud, this effective number clearly depends on the alignment of the PB with respect to the atomic cloud.

Let us suppose that the atomic cloud of total population N obeys a gaussian distribution centered at x_0:
$$N(x) = \frac{N}{\sqrt{\pi}\sigma}\exp[-(x-x_0)^2/\sigma^2]\ . \tag{3}$$
The transition rate for an atom at the position x inside the cloud to absorb a photon from the perturbing beam[1] of waist w_0 is given by:
$$S(X) = \frac{\Gamma}{2}\frac{I\exp\left[-2X^2/W_0^2\right]}{\Delta^2 + 1/4 + I\exp\left[-2X^2/W_0^2\right]} \tag{4}$$

[1] As the PB intensity is much higher than the intensity of the trap beams, we neglect the effect of the trapping beams in this calculation.

where we introduced the normalized variables:
$$I = I_P/I_S \tag{5}$$
$$X = x/\sigma \tag{6}$$
$$\Delta = \delta_P/\Gamma \tag{7}$$
$$W_0 = w_0/\sigma\ . \tag{8}$$
The total transition rate is thus given by:
$$\overline{S} = \frac{N}{\sqrt{8\pi}}\Gamma\ W_0\ e^{-X_0^2}F(Z) \tag{9}$$
where
$$F(Z) = Z\ e^{X_0^2}\int_{-\infty}^{+\infty} dy\ \exp\left[-\frac{W_0^2}{2}\left(y - \frac{\sqrt{2}X_0}{W_0}\right)^2\right] \times \frac{e^{-y^2}}{1+Ze^{-y^2}} \tag{10}$$
and
$$Z \equiv \frac{I}{\Delta^2 + 1/4}\ \cdot \tag{11}$$
Consider now the two terms under the integral sign. The first one is a displaced gaussian whose width is of the order of $W_0^{-1} \approx 100$, whereas the second is concentrated around $y = 0$. Thus:
$$F(Z) \approx Z\int_{-\infty}^{+\infty} dy\ \ \frac{e^{-y^2}}{1+Ze^{-y^2}}\cdot \tag{12}$$
We now write the loss term in equation (1) as
$$bN = b_0N + \frac{\sqrt{8\pi}}{\Gamma}\alpha\overline{S} = \left[b_0 + \alpha W_0\ e^{-X_0^2}\ F(Z)\right]N \tag{13}$$
where α is an unknown constant and the factor $\sqrt{8\pi}/\Gamma$ is introduced for later convenience. Let us define the scaled population variable $n = N/N_0$, with $N_0 = R/b_0$ being the unperturbed population of the trap and a scaled time $\tau = b_0t$. The equation of motion of the trap population (1) is then:
$$\frac{dn}{d\tau} = 1 - \left[1 + \alpha W_0\ e^{-X_0^2}\ F(Z)\right]n \tag{14}$$
and its stationary solution can be formally written as
$$n = \frac{1}{1 + \alpha W_0\ e^{-X_0^2}\ F(Z)}\cdot \tag{15}$$
If X_0 does not depend on the population of the trap, this equation gives the exact stationary solution for the trap population, which depends on the parameters of the PB

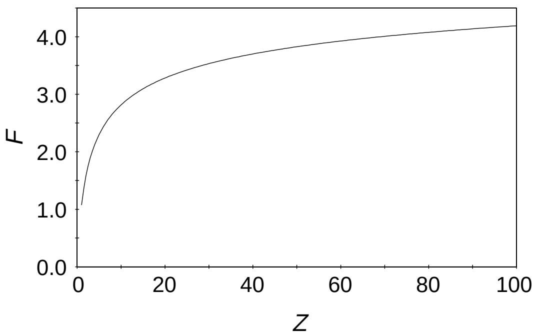

Fig. 7. The function $F(Z)$.

only through W_0 and Z. As Z is proportional to the intensity of the PB, it will give rise to a simple dependence of the population on the intensity of the beam, a curve starting from 1 as $I = 0$ and decreasing roughly with $1/I$, showing no bistability. However, a key feature of the system is the fact that position of the atomic cloud *depends* linearly on the population of the trap:

$$X_0 = an. \tag{16}$$

We can now invert equation (15) and obtain:

$$\beta F(Z) = \frac{1-n}{n}\exp(a^2n^2) \equiv G(n) \tag{17}$$

with $\beta \equiv \alpha \Gamma W_0$. A graphical representation of each side of this equation shows how bistability arises from the dependence of the position of the CM on the population of the cloud. In Figure 7 we plotted the function $F(Z)$ and in Figure 8 the function $G(n)$ for different values of the parameter a. A simple analysis then shows that the condition on the nonlinearity control parameter a to observe the bistability is:

$$a > (27/8)^{1/2} \simeq 1.84 \tag{18}$$

in which case $G(n)$ presents a maximum G_{max} and a minimum G_{min}. If this condition is satisfied, bistability should always arise: for a given value of β, it will show-up for some interval of Z values, $Z_\uparrow < Z < Z_\downarrow$, with the transition points satisfying $\beta F(Z_\uparrow) = G_{min}$ and $\beta F(Z_\downarrow) = G_{max}$.

Plotting the stationary value of n as a function of Z, one finds the usual structure of bistability, presenting two stable branches connected by an instable branch. Figure 9 shows a typical bistability cycle obtained from the above model.

In usual units, the relationship between the CM position and the population is $x_0 = \sigma a N/N_0$, which means that for a fully populated trap, the CM position is $x_0 = ar_{1/2}/\sqrt{\ln 2}$, where $r_{1/2}$ is the HWHM of the cloud. Experimentally, a precise measurement of the radius of a highly populated cloud is difficult because of its asymmetrical form (Fig. 4), but we observed that it is displaced with respect to the center of the trap of distance of the order of its diameter (1 mm); $a \simeq 2$ is thus a typical

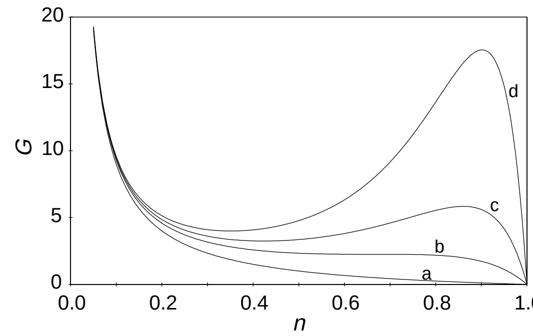

Fig. 8. The function $G(n)$ for different values of the parameter a. The general shape of the function changes for $a = 1.84$. For a greater than this threshold value, the function presents two local extrema, leading to the bistability. The values of a are (a) 0; (b) 1.84; (c) 2.0; (d) 2.2.

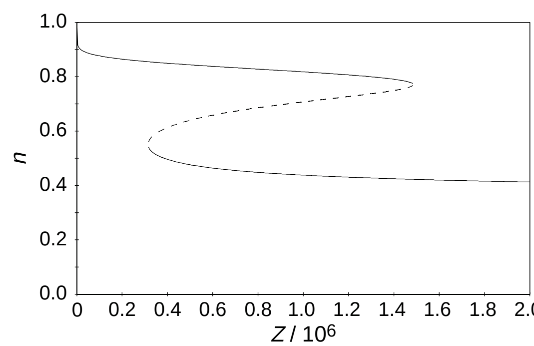

Fig. 9. Cycle of bistability obtained from the model developped above. The values of the parameters are $a = 1.916$ and $\alpha = 0.35$.

value (see Fig. 2). On the other hand, equation (13) allows us to write at the up-down turning point of the cycle, $b_\downarrow = b_0 + b_P = 1 + \alpha W_0\ e^{-X_0^2}\ F(Z_\downarrow)$, which implies

$$b_\downarrow/b_0 = 0.3 \tag{19}$$

for the parameters of Figure 9. The fact that the transition points of the bistability cycle correspond to a threshold value for the losses term will be used in the numerical model introduced in the next section.

In conclusion, we stress that the theoretical model presented above is useful to put into light the mechanism leading to the bistability phenomenon, but it cannot account for the exact interaction of the PB with the trapped atoms. A detailed comparison with the experimental data is thus not useful. In the next section, we present a more complete model of this interaction, considering the particular case of the up-down transition of the cycle. We will show that the confrontation of the calculations with the experimental measurements of the value of the $I_\downarrow$ transition point as a function of the detuning of the PB allows us to deduce the trap capture velocity along the PB.

4 Study of the interaction of the perturbing beam with the trapped atoms

The simple model we developed in the previous section brings us interesting information about the physical process underlying the bistability. In particular, the model suggests that the transitions observed in the bistability cycle correspond to threshold values of the losses induced by the perturbing beam. This idea is explored in the present section in order to construct a numerical model allowing us to calculate the transition intensity as a function of the detuning of the PB.

The interaction of the perturbing beam with the trapped atoms is a complex process. A cold atom inside the PB absorbs photons preferentially in this beam, because of its high intensity, and is thus accelerated. If it absorbs enough photons it is finally ejected from the trap. As a typical figure it should absorb thousands of photons before escaping the trap. Meanwhile, the atoms are moving and, as the high-intensity region inside the PB is spatially small, there is a chance for an atom to exit this region before escaping. However, as long as an atom stays inside the PB, its dynamics is dominated by this beam. We can thus simply modelize the trap effect in the direction of the PB as a square-well potential of depth $U = Mv_c^2/2$, where v_c is the capture velocity of MOT in the direction of the PB. The trapped atom evolves under the interaction with the PB and can eventually escape from the trap if its kinetic energy becomes larger than U. A numerical "classical Monte-Carlo" method simulates the motion of the atom inside the PB, and the comparison of the numerical simulation with experimental data allows us to deduce the trap capture velocity along the PB.

The capture velocity v_c of a magneto-optical trap is an important parameter. From simple arguments, one can deduce that the feeding rate R of the trap scales as $(v_c/\overline{v})^4$ where $\overline{v}$ is the mean velocity of the hot atoms feeding the trap [6]. However, due to the anisotropy of the trap, one easily understands that this velocity depends also on the direction of the motion of an atom entering the trapping region: if it is almost parallel to one of the trapping beams, it has greater chances of being captured than if its motion is parallel to the bisector of the trapping beams.

Our calculation is based in the following assumptions:

1. As mentioned above, the trap is modelized as a square-well potential, and thus described by a unique parameter, the capture velocity along the PB. An atom remains trapped as long as its velocity v is less than the capture velocity, otherwise it escapes from the trap. The capture velocity along the PB, $v_c(\theta)$, is the first parameter of the model.
2. Inside the region where the PB is intense, the rate of absorption of photons from the trap beams is negligeable as compared to the rate of absorption of photons from the PB.
3. As suggested by the model presented in the preceding section, we assume that the system shifts from its high-population state to its low-population state if the loss rate induced by the perturbing beam becomes greater than a threshold value $b_\downarrow$. Using equation (2), one sees that the transition condition $b_P > b_\downarrow$ corresponds to $N < N_\downarrow$, with

$$N_\downarrow = \frac{R}{b_0 + b_\downarrow} \simeq \frac{R}{b_0}\left(1 - \frac{b_\downarrow}{b_0}\right) = N_0\left(1 - \frac{b_\downarrow}{b_0}\right)\cdot \quad (20)$$

Let us introduce an easily accessible parameter, the depletion of the trap population, given by:

$$D \equiv 1 - \frac{N}{N_0}\cdot$$

The transition condition thus reads

$$D > D_\downarrow = \frac{b_\downarrow}{b_0 + b_\downarrow}\cdot$$

that will be the second parameter in our model.

In order to calculate the depletion of the trap, and so the transition intensity $I_\downarrow$, we performed a classical Monte-Carlo calculation. In this calculation we do not take into account the hyperfine structure of the Cesium, but we modelize it as a $J = 0 \rightarrow J = 1$ (that allows us to take into account the magneto-optical trapping effect), with a dipole matrix element equal to the mean value for cesium. This is one of the limitations of the model. We take into account the motion along the PB (x' direction, see Fig. 1) and the transverse motion with respect to this beam (y' direction). We suppose that there is a perfect symmetry in the plane orthogonal to the direction of propagation of the PB. This is justified by the high intensity of the PB, that dominates the dynamics of the atoms inside it. The fact, verified by the numerical simulation, that the typical number of fluorescence cycles necessary to expel an atom from the trap is a few thousands[2], implies that the global effect of the spontaneous emitted photon on the atomic motion averages to zero[3] and can be neglected in our calculation. Our model takes into account the light-shift due to the PB intensity and the effect of the intensity-gradient (dipole) force on the motion of the atom. We let the atom evolve along the PB until one of the following conditions is fulfilled:

a) If the velocity of the atom becomes greater than the capture velocity the atom is expelled from the trap.
b) If the transverse motion of the atom takes it outside the PB, the atom remains trapped. In order to precisely decide when the atom exits the PB, we calculate

[2] This can also be seen by an order of magnitude argument. The change in the atomic velocity corresponding to the absorption of a photon is 3.5 mm/s. The capture velocity, as we find below, is of order of tenths of meter per second. Thus the number of absorptions needed to accelerate an atom from rest to the velocity of capture is roughly ten thousand.

[3] In fact, we performed a limited number of simulations in which the full degrees of freedom of the atomic motion were taken into account. It is a time-consuming calculation, and the results obtained were in good agreement with the simplified model described above.

the photon absorption transition rate given by equation (4), whose maximum value is $S_{max} = \Gamma/2$. We consider that the atom is outside the PB at the position x if $S(x) < \eta S_{max}$, for a given threshold value η. We numerically verified that the results are not affected if η is decreased. In our calculations we used $\eta = 0.01$.

For each value of the angle θ, we have a set of experimental data (see Fig. 6) $I_{\downarrow}^{exp}(\Delta_P^i)$ for different values Δ_P^i of the detuning of the PB. We use the numerical model to calculate these values. The calculation proceeds as follows. For fixed values of v_c, I_P, Δ_P^i, we start from a sample of atoms (2.5×10^4) chosen in order to satisfy the spatial and velocity distributions corresponding to the atomic cloud features. We let the system evolve and we calculate the value of the cloud depletion $D(v_c, I_P, \Delta_P^i)$. We choose a threshold value for the depletion corresponding to the up-low transition, $D_{\downarrow}$, and we adjust the PB intensity to a value $I_{\downarrow}^i$ such that $D(v_c, I_{\downarrow}^i, \Delta_P^i) = D_{\downarrow}$. We repeat the procedure for all values of the PB detuning corresponding to the set of experimental data, which produces a set of theoretical values $I_{\downarrow}^{th}(v_c, D_{\downarrow}, \Delta_P^i)$. The error function $\varepsilon(v_c, D_{\downarrow}) = \sum_i \left| I_{\downarrow}^{th}(v_c, D_{\downarrow}, \Delta_P^i) - I_{\downarrow}^{exp}(\Delta_P^i) \right|$ is then minimized by adjusting v_c and $D_{\downarrow}$. This is gives us the best (two-parameter) fit to the experimental data corresponding to the full line in Figure 6. The comparison with the experimental data shows a reasonable agreement.

The value obtained for $D_{\downarrow} = 0.25 \pm 0.02$ is the same for the two sets of data, which confirms that the condition for the transition is a threshold depletion of the trap by the PB, in agreement with the prediction of the model discussed in the previous section, equation (19): $b_{\downarrow}/b_0 = 0.3 \Longrightarrow D_{\downarrow} = 0.23$. This result is physically evident if one remarks that the transition occurs when the displacement of the cloud with respect to the center of the trap (and thus with the center of the PB) becomes small enough, which corresponds to a threshold value for the optical thickness of the cloud. On the other hand, as expected, the value for the capture velocity we obtained strongly depends on the value of the angle θ that the PB makes with the arms of the trap: $v_c(23°) = 49 \pm 3$ m/s and $v_c(35°) = 12 \pm 2$ m/s. The uncertainties are almost equally due to the experimental uncertainty and to the numerical simulation. The obtained values show that the magneto-optical trap is more efficient in slowing and capturing atoms that enters it along one of its arms than in trapping atoms that enters it along a bisector.

Measurements of the *mean* value of the capture velocity have been reported in the literature in a variety of situations and for a large range of parameters. The reported values range from 35 m/s [7] to 11 m/s [8].

Unfortunately, the geometry of our MOT prevents us from making measurements for very small angles or for angles very close to the bisector, which would be very interesting in order to give us an idea of the functional dependence of the capture velocity on the angle θ. Nevertheless, the results presented above show that the study of the bistability cycles obtained with the experimental scheme described in this paper is a powerful method to study the capture properties of the MOT.

5 Conclusion

The bistability phenomenon presented above originates from the non-linearity due to the coupling between the displacement produced by the *shadow effect* and the population of the magneto-optical trap. This effect is related to the usual MOT configuration, namely three orthogonal arms formed each one by a retro-reflected laser beam. This configuration is by far the most common one; yet its dynamical properties have been astonishingly seldom studied in detail. The results presented here are intended to be a step in the comprehension of the complex dynamics of the MOT atomic cloud, allowing the study of its basic mechanism: the ability for capturing and trapping atoms.

The authors are indebted to G. Grynberg, S. Guibal, C. Salomon and P. Verkerk, for many fruitful discussions and help with the set-up of the magneto-optical trap. P. Szriftgiser is also acknowledged for interesting discussions and suggestions. Centre d'Études et Recherches Lasers et Applications (CERLA) is supported by Ministère de la Recherche, Région Nord-Pas de Calais and Fonds Européen de Développement Économique des Régions.

References

1. J. Dalibard, C. Cohen-Tannoudji, J. Opt. Soc. Am. B **6**, 2023 (1989).
2. T. Walker, D. Sesko, C. Wieman, Phys. Rev. Lett. **64**, 408 (1990).
3. D.W. Sesko, T.G. Walker, C. Monroe, A. Gallagher, C.E. Wieman, Phys. Rev. Lett. **63**, 961 (1989).
4. D.W. Sesko, T.G. Walker, C.E. Wieman, J. Opt. Soc. Am. B **8**, 946 (1991).
5. V.S. Bagnato, L.G. Marcassa, M. Oria, G.I. Surdutovich, R. Vitlina, S.C. Zilio, Phys. Rev. A **48**, 3771 (1993); I. Guedes, M.T. Araujo, D.M.P. Milori, G.I. Surdutovich, V.S. Bagnato, S.C. Zilio, J. Opt. Soc. Am. B **11**, 1935 (1994).
6. C. Monroe, W. Swann, H. Robinson, C. Wieman, Phys. Rev. Lett. **62**, 1571 (1990).
7. K.E. Giblle, S. Kasapi, S. Chu, Opt. Lett. **17**, 526 (1992).
8. K. Lindquist, M. Stephens, C. Wieman, Phys. Rev. A. **46**, 4082 (1992).
9. Z. Hu, H.J. Kimble, Opt. Lett. **19**, 1888 (1994); P.A. Willemens, R.A. Boyd, J.L. Bliss, K.G. Libbrecht, Phys. Rev. Lett. **78**, 1660 (1997).